



Measurement of electrons from beauty hadron decays in pp collisions at $\sqrt{s} = 7$ TeV

ALICE Collaboration

ARTICLE INFO

Article history:

Received 29 October 2012
 Received in revised form 30 January 2013
 Accepted 31 January 2013
 Available online 9 February 2013
 Editor: W.-D. Schlatter

Keywords:

LHC
 ALICE experiment
 pp collisions
 Single electrons
 Heavy flavor production
 Beauty production

ABSTRACT

The production cross section of electrons from semileptonic decays of beauty hadrons was measured at mid-rapidity ($|y| < 0.8$) in the transverse momentum range $1 < p_T < 8$ GeV/c with the ALICE experiment at the CERN LHC in pp collisions at a center of mass energy $\sqrt{s} = 7$ TeV using an integrated luminosity of 2.2 nb^{-1} . Electrons from beauty hadron decays were selected based on the displacement of the decay vertex from the collision vertex. A perturbative QCD calculation agrees with the measurement within uncertainties. The data were extrapolated to the full phase space to determine the total cross section for the production of beauty quark–antiquark pairs.

© 2013 CERN. Published by Elsevier B.V. Open access under CC BY-NC-ND license.

The measurement of heavy-flavor (charm and beauty) production in proton–proton (pp) collisions at the CERN Large Hadron Collider (LHC) provides a crucial testing ground for quantum chromodynamics (QCD), the theory of strong interactions, in a new high-energy regime. Because of their large masses heavy quarks are mainly produced via initial hard parton–parton collisions, even at low transverse momenta p_T . Therefore, heavy-flavor production cross sections constitute a prime benchmark for perturbative QCD (pQCD) calculations. Furthermore, heavy-flavor measurements in pp collisions provide a mandatory baseline for corresponding studies in nucleus–nucleus collisions. Heavy quark observables are sensitive to the properties of the strongly interacting partonic medium which is produced in such collisions.

Earlier measurements of beauty production in $p\bar{p}$ collisions at $\sqrt{s} = 1.96$ TeV at the Tevatron [1] are in good agreement with pQCD calculations at fixed order with next-to-leading log resummation (FONLL) [2,3]. Measurements of charm production, available at high p_T only [4], are close to the upper limit but still consistent with such pQCD calculations. The same trend was observed in pp collisions at $\sqrt{s} = 0.2$ TeV at RHIC [5,6].

In pp collisions at the LHC, heavy-flavor production was investigated extensively at $\sqrt{s} = 7$ TeV in various decay channels. With LHCb beauty hadron production cross sections were measured at forward rapidity [7] and, at high p_T only, with CMS at mid-rapidity [8]. At low p_T , mid-rapidity J/ψ meson production from beauty hadron decays was studied with ALICE [9]. These

results, as well as the mid-rapidity D-meson production cross sections measured with ALICE [10], are well described by FONLL pQCD calculations. The same is true for the production cross sections of electrons and muons from semileptonic decays of heavy-flavor hadrons reported by ATLAS [11] at high p_T , and by ALICE down to low p_T [12,13]. However, still missing at the LHC is the separation of leptons from charm and beauty hadron decays at low p_T , which is important for the total beauty production cross section and which provides a crucial baseline for Pb–Pb collisions.

This Letter reports the mid-rapidity ($|y| < 0.8$) production cross section of electrons, $(e^+ + e^-)/2$, from semileptonic beauty hadron decays measured with the ALICE experiment in the range $1 < p_T < 8$ GeV/c in pp collisions at $\sqrt{s} = 7$ TeV. Two independent techniques were used for the separation of beauty hadron decay electrons from those originating from other sources, in particular charm hadron decays. The resulting invariant cross sections of electrons from beauty and from charm hadron decays are compared with corresponding predictions from a FONLL pQCD calculation. In addition, the measured cross sections were extrapolated to the full phase space and the total beauty and charm production cross sections were determined.

The data set used for this analysis was recorded during the 2010 LHC run with ALICE, which is described in detail in [14]. Charged particle tracks were reconstructed in the pseudorapidity range $|\eta| < 0.8$ with the Time Projection Chamber (TPC) and the Inner Tracking System (ITS) which, in addition, provides excellent track spatial resolution at the interaction point. Electron candidates were selected with the TPC and the Time-Of-Flight detector (TOF). Data were collected using a minimum bias (MB) trigger [12]

derived from the VZERO scintillator arrays and the Silicon Pixel Detector (SPD), which is the innermost part of the ITS consisting of two cylindrical layers of hybrid silicon pixel assemblies. The MB trigger cross section $\sigma_{\text{MB}} = 62.2 \pm 2.2 \text{ mb}$ [15] was measured in a van-der-Meer scan. An integrated luminosity of 2.2 nb^{-1} was used for this analysis.

Pile-up events were identified by requiring no more than one primary vertex to be reconstructed with the SPD as discussed in [12]. Taking into account the efficiency of the pile-up event identification, only 2.5% of the triggered events suffered from pile-up. The corresponding events were removed from the analyzed data sample. The systematic uncertainty due to the remaining undetected pile-up events was negligible.

Events and tracks were selected following the approach from a previous analysis [12]. Charged particle tracks reconstructed in the TPC and ITS were propagated towards the outer detectors using a Kalman filter approach [16]. Geometrical matching was applied to associate tracks with hits in the outer detectors. To guarantee good particle identification based on the specific dE/dx in the TPC, tracks were required to include a minimum number of 80 clusters used for the energy loss calculation. A cut on the number of clusters for tracking is used to enhance the electron/pion separation. The stringent request for at least 120 clusters from the maximum of 159 enhances electrons relative to hadrons. In total, at least four ITS hits were required to be associated with a track. A cut on the distance of closest approach (DCA) to the primary vertex in the plane perpendicular to the beam axis (xy) as well as in the beam direction (z) was applied to reject background tracks and non-primary tracks. Differently from the heavy-flavor electron analysis [12], the pseudorapidity range was extended to $|\eta| < 0.8$, and tracks were required to be associated with hits in both layers of the SPD in order to minimize the contribution from tracks with randomly associated hits in the first pixel layer. The latter criterion provides a better measurement of the track's transverse impact parameter d_0 , i.e. the DCA to the primary collision vertex in the plane perpendicular to the beam axis, where the sign of d_0 is attributed on the basis of the relative position of primary vertex and the track prolongation in the direction perpendicular to the direction of the transverse momentum vector of the track.

Electron candidates were required to be consistent within three standard deviations with the electron time of flight hypothesis, thus efficiently rejecting charged kaon background up to momenta of $\approx 1.5 \text{ GeV}/c$ and proton background up to $\approx 3 \text{ GeV}/c$. Additional background, in particular from charged pions, was rejected using the specific energy loss, dE/dx , measured for charged particles in the TPC.

Due to their long lifetime ($c\tau \sim 500 \mu\text{m}$), beauty hadrons decay at a secondary vertex displaced in space from the primary collision vertex. Consequently, electron tracks from semileptonic beauty hadron decays feature a rather broad d_0 distribution, as indicated by simulation studies in Fig. 1(a). Also shown are the d_0 distributions of the main background sources, i.e. electrons from charm hadron decays, from Dalitz and dilepton decays of light mesons, and from photon conversions. These distributions were obtained from a detailed Monte Carlo simulation of the experiment using GEANT3 [17]. With the PYTHIA 6.4.21 event generator [18] pp collisions were produced employing the Perugia 0-parameter tuning [19]. The p_T shapes of beauty hadron decay electrons from a FONLL pQCD calculation [20] and from PYTHIA are in good agreement. The PYTHIA simulation does not reproduce precisely the p_T -differential yields of background sources measured in data. Therefore, the p_T distributions of the relevant electron sources in PYTHIA were re-weighted to match the distributions measured with ALICE, prior of propagation through the ALICE apparatus using GEANT3. After the full Monte Carlo simulation, the same event

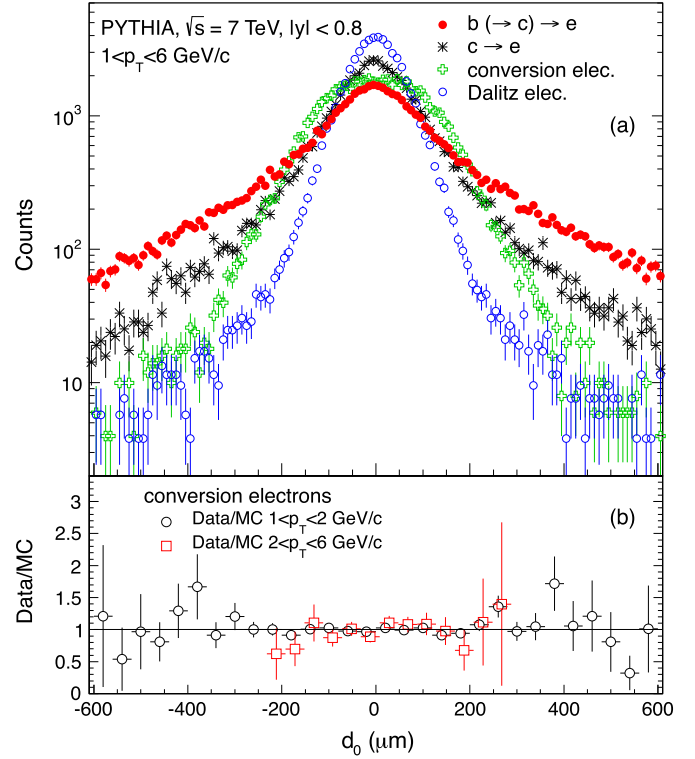


Fig. 1. (Color online.) (a) d_0 distributions of electrons from beauty and charm hadron decays as well as from photon conversions obtained from PYTHIA simulations in the electron p_T range $1 < p_T < 6 \text{ GeV}/c$. The distributions were normalized to the same integrated yield. (b) Ratios of the measured and the simulated d_0 distributions of conversion electrons in the ranges $1 < p_T < 2 \text{ GeV}/c$ and $2 < p_T < 6 \text{ GeV}/c$ (points shifted in d_0 by $10 \mu\text{m}$ for better visibility).

cuts and track selection criteria (including that on d_0) as in data were applied. The p_T distributions of the backgrounds were normalized by the number of events passing these event selection cuts, corrected for the efficiency to reconstruct a primary vertex. Background electrons surviving these selection criteria were subtracted from the inclusive electron spectrum obtained from data. This approach relies on the availability of the p_T -differential cross section measurements of the main background sources.

The production cross sections of π^0 and η mesons, the dominant sources of electrons from Dalitz decays and from photons which convert in material into e^+e^- pairs, were measured with ALICE in pp collisions at $\sqrt{s} = 7 \text{ TeV}$ [21]. The conversion electron yield depends on the material budget which was measured with a systematic uncertainty of 4.5% [21]. Other light hadrons and heavy quarkonia contribute through their decays to the electron spectrum and their phase space distributions were calculated with the approach described in [12]. This calculation also includes real and virtual photon production via partonic hard scattering processes. D^0 , D^+ , and D_s^+ meson production cross sections were measured with ALICE [10,22] in the transverse momentum ranges $1 < p_T < 16 \text{ GeV}/c$, $1 < p_T < 24 \text{ GeV}/c$, and $2 < p_T < 12 \text{ GeV}/c$, respectively. Based on a FONLL pQCD calculation [20] the measured p_T -differential cross sections were extrapolated to $p_T = 50 \text{ GeV}/c$. The contribution from the unmeasured high- p_T region to the electron yield from D-meson decays was estimated to be $\leq 10\%$ for electrons with $p_T < 8 \text{ GeV}/c$. A contribution from Λ_c decays was included using a measurement of the ratio $\sigma(\Lambda_c)/\sigma(D^0 + D^+)$ from ZEUS [23].

The measured p_T spectra of the main background sources drop more quickly with p_T than the ones generated by PYTHIA for

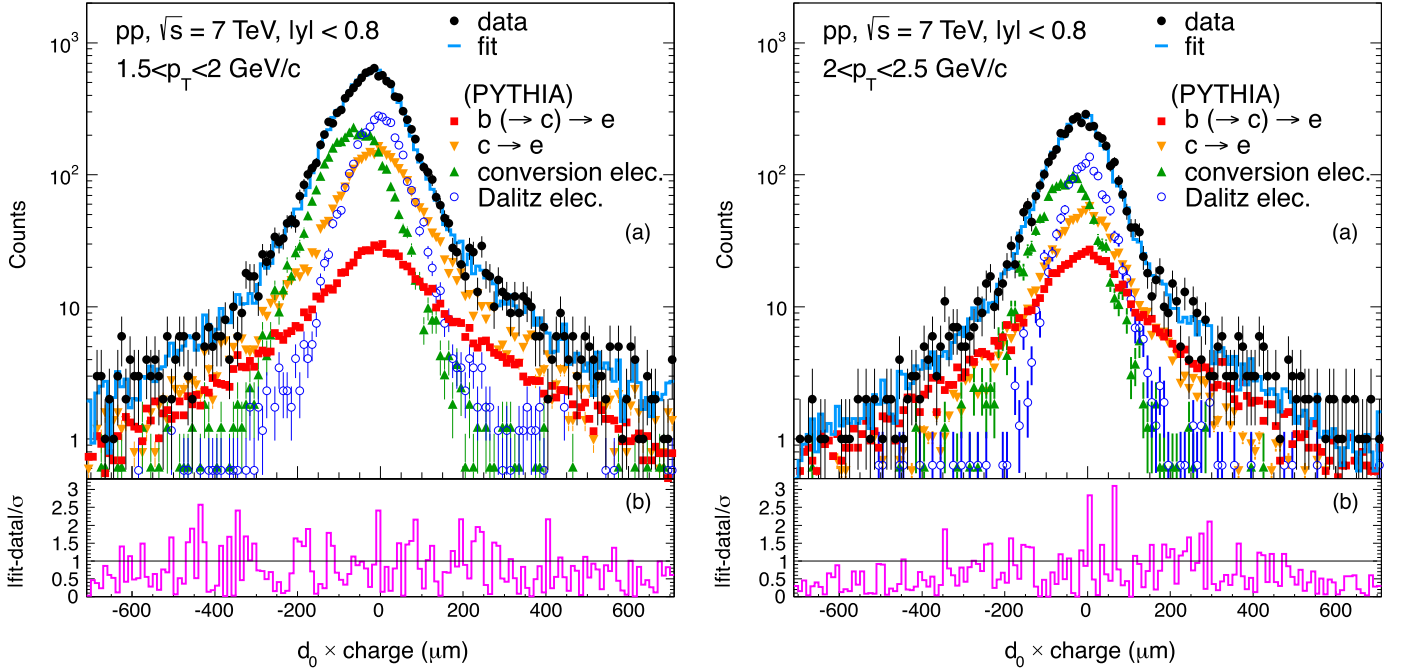


Fig. 2. (Color online.) (a) Distribution of $d_0 \times \text{charge}$ for electron candidates after all analysis cuts (except that on d_0) superimposed to the best-fit result. The fit function is defined as the sum of the Monte Carlo d_0 distribution of beauty electrons and those of electrons from all other sources, the normalizations being the free parameters in the fit. The error bars represent the statistical uncertainties. (b) Differences between the data and the best fit result divided by the statistical error.

$p_T > 1 \text{ GeV}/c$. The ratio of the measured yield and the yield from PYTHIA, which was used to weight the spectra of the electron sources in PYTHIA, is 1.3 (0.6) at $p_T = 1(10) \text{ GeV}/c$ for π^0 . The corresponding ratio is 2.4 (1.3) at $p_T = 1(10) \text{ GeV}/c$ for η mesons, and 0.95 (0.2) at $p_T = 1(10) \text{ GeV}/c$ for electrons from charm hadron decays.

A cut on the d_0 parameter is applied in order to enhance the signal-to-background ratio (S/B) of electrons from beauty hadron decays. For this, it is crucial that the d_0 resolution is properly reproduced in the simulation. The d_0 resolution is found to be $80 \mu\text{m}$ ($30 \mu\text{m}$) for tracks with $p_T = 1(10) \text{ GeV}/c$ [10]. The agreement of the d_0 measurement of electron candidates with the simulation is demonstrated in Fig. 1(b), which shows the ratios of the measured d_0 distribution to the one from simulation in the p_T ranges $1 < p_T < 2 \text{ GeV}/c$ and $2 < p_T < 6 \text{ GeV}/c$ for electrons from photon conversions, which is the only identifiable source in data. A pure sample of electrons from photon conversions in the detector material was identified using a V0-finder and topological cuts [24]. At $p_T > 6 \text{ GeV}/c$, the number of reconstructed conversions was statistically insufficient for this cross check. In addition, the d_0 resolution measured for charged tracks in data is reproduced within 10% by the Monte Carlo simulation [10]. The difference in the particle multiplicities between data and simulation gives an effect on the primary vertex resolution, which is included in the d_0 resolution as a convolution of the track position and the primary vertex resolution. The Monte Carlo simulation shows that the electron Bremsstrahlung effect is limited to transverse momenta below $1 \text{ GeV}/c$. At higher p_T , the particle species dependences of the d_0 resolution is negligible.

Fig. 2 shows that the d_0 distribution of the data sample is well described by the cocktail of signal and background. The measured d_0 distribution of identified electrons was fitted by minimizing a χ^2 between the measured d_0 distribution and the sum of the Monte Carlo d_0 distributions of signal and background in the corresponding electron p_T range. The differences between the data and the cocktail are consistent with statistical variations. The ra-

tio of the signal to background yields, which is obtained by this fit procedure, agrees with that obtained in the present analysis within statistical uncertainties.

The widths of the d_0 distributions depend on p_T . Only electrons satisfying the condition $|d_0| > 64 + 780 \times \exp(-0.56p_T)$ (with d_0 in μm and p_T in GeV/c) were considered for the further analysis. This p_T -dependent d_0 cut was determined from the simulation to maximize the significance for the beauty decay electron spectrum. The possible bias introduced by this optimization is taken into account in the estimation of the systematic uncertainties, by varying substantially the cut value.

Fits of the TPC dE/dx distribution in momentum slices indicate that the remaining hadron contamination grows from less than 10^{-5} at $1 \text{ GeV}/c$ to $\approx 20\%$ at $8 \text{ GeV}/c$ before the application of the d_0 cut. Since hadrons originate from the primary collision vertex, the latter cut reduces the remaining hadron contamination to less than 3% even at the highest p_T considered here. The electron background from sources other than beauty hadron decays was estimated based on the method described above. In Fig. 3 the raw electron yield, as well as the non-beauty electron background yield, which is subtracted in the analysis, are shown after the application of the track selection criteria. At $p_T = 1 \text{ GeV}/c$, the background contributions from charm hadron decays, light meson decays, and photon conversions are approximately equal and S/B is $\approx 1/3$. At $p_T = 8 \text{ GeV}/c$, the background originates mostly from charm hadron decays and S/B is ≈ 5 .

The electron yield from beauty hadron decays, $N_e(p_T)$, was corrected for the geometrical acceptance, the track reconstruction efficiency, the electron identification efficiency, and the efficiency of the d_0 cut. The total efficiency ε is the product of these individual factors. ε was computed from a full detector simulation using GEANT3 as discussed in [12]. In addition, the electron p_T distribution was corrected for effects of finite momentum resolution and energy loss due to Bremsstrahlung via a p_T unfolding procedure which does not depend on the p_T shape of Monte Carlo simulation [12].

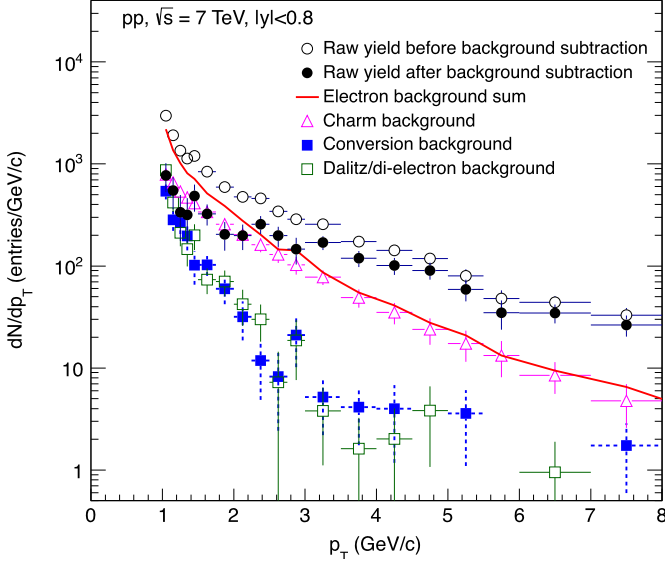


Fig. 3. (Color online.) The signal (black solid circle) and the background yields after the application of the track selection criteria including the one on d_0 . The background electrons (red solid line), i.e. the sum of the electrons from charm hadron decays, from Dalitz and dilepton decays of light mesons, and from photon conversions, were subtracted from the inclusive electron spectrum (black open circle). The error bars represent the statistical uncertainties. The symbols are plotted at the center of each bin.

The invariant cross section of electron production from beauty hadron decays in the range $|y| < 0.8$ was then calculated using the corrected electron p_T spectrum, the number of minimum bias pp collisions N_{MB} , and the minimum bias cross section σ_{MB} as

$$\frac{1}{2\pi p_T} \frac{d^2\sigma}{dp_T dy} = \frac{1}{2\pi p_T^c} \frac{N_e(p_T)}{\Delta y \Delta p_T} \frac{1}{\varepsilon N_{MB}} \sigma_{MB}, \quad (1)$$

where p_T^c are the centers of the p_T bins with widths Δp_T and $\Delta y = 0.8$ is the width of the rapidity interval.

A summary of the estimated relative systematic uncertainties is provided in Table 1. The systematic uncertainties for the tracking and the particle identification are the following: the corrections of the ITS, TPC, TOF tracking efficiencies, the TOF, TPC particle identification efficiencies, the p_T unfolding procedure. These amount to $^{+17}_{-14}$ ($^{+8}_{-14}$)% for $p_T < (>) 3$ GeV/c. Additional systematic uncertainties specific for this analysis due to the d_0 cut, the subtraction of the light hadron decay background and charm hadron decay background were added in quadrature. The systematic uncertainty induced by the d_0 cut was evaluated by repeating the full analysis with modified cuts. The variation of this cut was chosen such that it corresponds to $\pm 1\sigma$, where σ is the d_0 resolution measured on data [10]. These vary the minimum d_0 cut efficiency by $\pm 20\%$. In addition, the full analysis was repeated after smearing the d_0 resolution in the Monte Carlo simulation by 10% [10], considering the maximum differences in the d_0 distribution in data and simulation. The uncertainty due to the background subtraction was evaluated by propagating the statistical and systematic uncertainties of the light and charm hadron measurements used as analysis input. At low p_T , the uncertainties are dominated by the subtraction of charm hadron decay background.

Fig. 4 presents the invariant production cross section of electrons from beauty hadron decays obtained with the analysis based on the d_0 cut. As a cross check the corresponding result from an alternative method is shown. In the latter, the decay electron spectrum was calculated for charm hadrons as measured with ALICE [10] based on a fast Monte Carlo simulation using PYTHIA decay kinematics, and it was subtracted from the electron spectrum

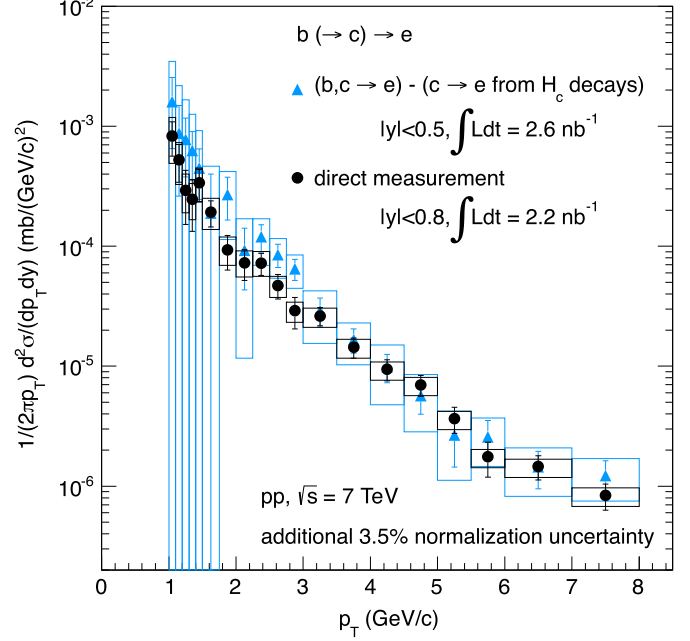


Fig. 4. (Color online.) Invariant cross sections of electrons from beauty hadron decays measured directly via the transverse impact parameter method and indirectly via subtracting the calculated charm hadron decay contribution from the measured heavy-flavor hadron decay electron spectrum [12]. The error bars (boxes) represent the statistical (systematic) uncertainties.

Table 1

Overview of the contributions to the systematic uncertainties. The total systematic uncertainty is calculated as the quadratic sum of all contributions.

p_T range (GeV/c)	1–8
Error source	Systematic uncertainty [%]
Track matching	± 2
ITS number of hits	± 1 -4
TPC number of tracking clusters	$^{+15}_{-7}$ ($^{+3}_{-4}$) for $p_T < 2.5 (> 2.5)$ GeV/c
TPC number of PID clusters	± 2
DCA to primary vertex in xy (z)	± 1
TOF matching and PID	± 5
TPC PID	$^{+15}_{-5}$ ($^{+2}_{-5}$) for $p_T < 3 (> 3)$ GeV/c
Minimum d_0 cut	± 12
Charge dependence	± 1 -7
η dependence	-6
Unfolding	± 5
Light hadron decay background	$\approx 10 (< 2)$ for $p_T = 1 (> 2)$ GeV/c
Charm hadron decay background	$\approx 30 (< 10)$ for $p_T = 1 (> 3)$ GeV/c

measured for all heavy-flavor hadron decays [12]. The systematic uncertainties of these two inputs have been added in quadrature as they are uncorrelated. The results from the subtraction method, which does not use a d_0 cut, and from the analysis based on the d_0 selection agree within the experimental uncertainties, which are much smaller, in particular at low p_T , for the beauty measurement employing the d_0 cut.

In Fig. 5(a) FONLL pQCD predictions [20] of the electron production cross sections are compared with the measured electron spectrum from beauty hadron decays and with the calculated electron spectrum from charm hadron decays. The ratios of the measured cross sections to the FONLL predictions are shown in Figs. 5(b) and 5(c) for electrons from beauty and charm hadron decays, respectively. The FONLL predictions are in good agreement with the data. At low p_T , electrons from heavy-flavor hadron decays originate predominantly from charm hadrons. As demonstrated in Fig. 5(d), beauty hadron decays take over from charm as the dominant

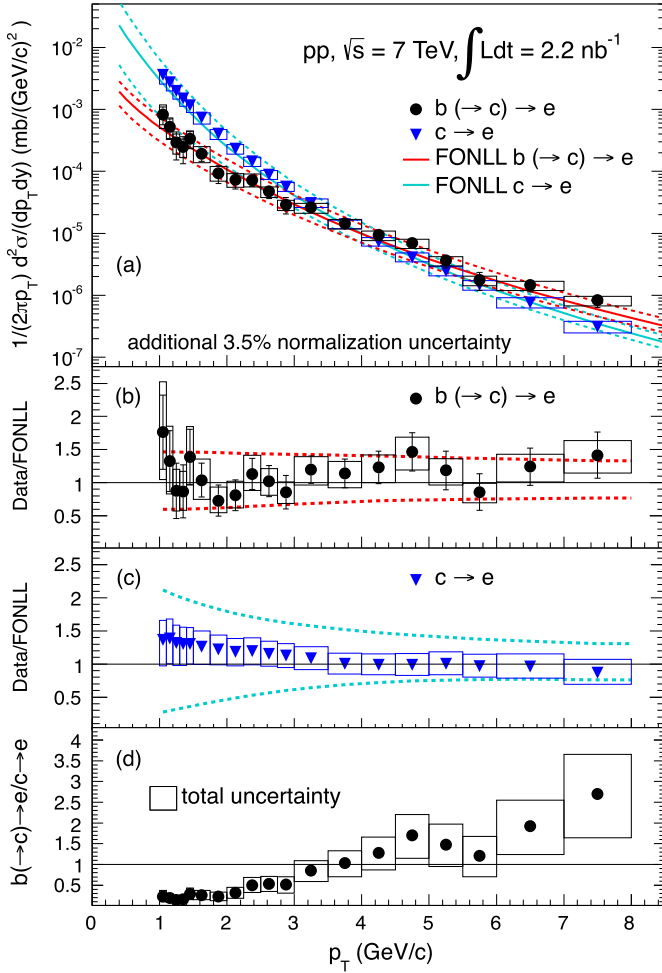


Fig. 5. (Color online.) (a) p_T -differential invariant cross sections of electrons from beauty and from charm hadron decays. The error bars (boxes) represent the statistical (systematic) uncertainties. The solid (dashed) lines indicate the corresponding FONLL predictions (uncertainties) [20]. Ratios of the data and the FONLL calculations are shown in (b) and (c) for electrons from beauty and charm hadron decays, respectively, where the dashed lines indicate the FONLL uncertainties. (d) Measured ratio of electrons from beauty and charm hadron decays with error boxes depicting the total uncertainty.

source of electrons from heavy-flavor hadron decays close to electron transverse momenta of 4 GeV/c .

The integrated cross section of electrons from beauty hadron decays was measured as $6.61 \pm 0.54(\text{stat})_{-1.86}^{+1.92}(\text{sys}) \mu\text{b}$ for $1 < p_T < 8 \text{ GeV}/c$ in the range $|y| < 0.8$. The beauty production cross section $\sigma_{b\bar{b}}$ was calculated by extrapolating this p_T -integrated visible cross section down to $p_T = 0$ and to the full y range. The extrapolation factor was determined based on FONLL as described in [9], using the beauty to electron branching ratio $\text{BR}_{H_b \rightarrow e} + \text{BR}_{H_b \rightarrow H_c \rightarrow e} = 0.205 \pm 0.007$ [25]. The related uncertainty was obtained as the quadratic sum of the uncertainties from the beauty quark mass, from perturbative scales, and from the CTEQ6.6 parton distribution functions [26]. At mid-rapidity the beauty production cross section per unit rapidity is $d\sigma_{b\bar{b}}/dy = 42.3 \pm 3.5(\text{stat})_{-11.9}^{+12.3}(\text{sys})_{-1.7}^{+1.1}(\text{extr}) \mu\text{b}$, where the additional systematic uncertainty due to the extrapolation procedure is quoted separately. The total cross section was derived as $\sigma_{b\bar{b}} = 280 \pm 23(\text{stat})_{-79}^{+81}(\text{sys})_{-8}^{+7}(\text{extr}) \pm 10(\text{BR}) \mu\text{b}$, consistent with the result of a previous measurement of J/ψ mesons from beauty hadron decays $\sigma_{b\bar{b}} = 282 \pm 74(\text{stat})_{-68}^{+58}(\text{sys})_{-7}^{+3}(\text{extr}) \mu\text{b}$ [9]. The weighted average of the two measurements was calculated based

on the procedure described in [27]. The statistical and systematic uncertainties of two measurements are largely uncorrelated, but the extrapolation uncertainties using the same theoretical model (FONLL) are correlated. The weights, defined using the statistical and the uncorrelated systematic uncertainties, and the correlated extrapolation uncertainties, are calculated as 0.499 for the measurement using semileptonic beauty hadron decays and 0.501 for that using non-prompt J/ψ mesons. The combined total cross section is $\sigma_{b\bar{b}} = 281 \pm 34(\text{stat})_{-54}^{+53}(\text{sys})_{-8}^{+7}(\text{extr}) \mu\text{b}$. FONLL predicts $\sigma_{b\bar{b}} = 259_{-96}^{+120} \mu\text{b}$ [20].

The production cross section of electrons from heavy-flavor hadron decays was measured as $37.7 \pm 3.2(\text{stat})_{-14.4}^{+13.3}(\text{sys}) \mu\text{b}$ for $0.5 < p_T < 8 \text{ GeV}/c$ in the range $|y| < 0.5$ [12]. After subtraction of the contribution from beauty hadron decays (see above) the resulting production cross section of electrons from charm hadron decays was converted into a charm production cross section applying the same extrapolation method as for beauty. With the branching ratio $\text{BR}_{H_c \rightarrow e} = 0.096 \pm 0.004$ [25], at mid-rapidity the charm production cross section per unit rapidity is $d\sigma_{c\bar{c}}/dy = 1.2 \pm 0.2(\text{stat}) \pm 0.6(\text{sys})_{-0.1}^{+0.2}(\text{extr}) \text{mb}$. The total cross section $\sigma_{c\bar{c}} = 10.0 \pm 1.7(\text{stat})_{-5.5}^{+5.1}(\text{sys})_{-0.5}^{+3.5}(\text{extr}) \pm 0.4(\text{BR}) \text{mb}$ is consistent with the result of a previous, more accurate measurement using D mesons $\sigma_{c\bar{c}} = 8.5 \pm 0.5(\text{stat})_{-2.4}^{+1.0}(\text{sys})_{-0.4}^{+5.0}(\text{extr}) \text{mb}$ [28]. The FONLL prediction is $\sigma_{c\bar{c}} = 4.76_{-3.25}^{+6.44} \text{mb}$ [20]. All measured cross sections have an additional normalization uncertainty of 3.5% [15].

In summary, invariant production cross sections of electrons from beauty and from charm hadron decays were measured in pp collisions at $\sqrt{s} = 7 \text{ TeV}$. The agreement between theoretical predictions and the data suggests that FONLL pQCD calculations can reliably describe heavy-flavor production even at low p_T in the highest energy hadron collisions accessible in the laboratory today. Furthermore, these results provide a crucial baseline for heavy-flavor production studies in the hot and dense matter created in Pb–Pb collisions at the LHC.

Acknowledgements

The ALICE Collaboration would like to thank all its engineers and technicians for their invaluable contributions to the construction of the experiment and the CERN accelerator teams for the outstanding performance of the LHC complex. The ALICE Collaboration would like to thank M. Cacciari for providing the FONLL pQCD predictions for the cross sections of electrons from heavy-flavour hadron decays. The ALICE Collaboration acknowledges the following funding agencies for their support in building and running the ALICE detector: State Committee of Science, Calouste Gulbenkian Foundation from Lisbon and Swiss Fonds Kidagan, Armenia; Conselho Nacional de Desenvolvimento Científico e Tecnológico (CNPq), Financiadora de Estudos e Projetos (FINEP), Fundação de Amparo à Pesquisa do Estado de São Paulo (FAPESP); National Natural Science Foundation of China (NSFC), the Chinese Ministry of Education (CMOE) and the Ministry of Science and Technology of China (MSTC); Ministry of Education and Youth of the Czech Republic; Danish Natural Science Research Council, the Carlsberg Foundation and the Danish National Research Foundation; The European Research Council under the European Community's Seventh Framework Programme; Helsinki Institute of Physics and the Academy of Finland; French CNRS-IN2P3, the 'Region Pays de Loire', 'Region Alsace', 'Region Auvergne' and CEA, France; German BMBF and the Helmholtz Association; General Secretariat for Research and Technology, Ministry of Development, Greece; Hungarian OTKA and National Office for Research and Technology (NKTH); Department of Atomic Energy and Department of Science and Technology of the Government of India; Istituto Nazionale di

Fisica Nucleare (INFN) and Centro Fermi – Museo Storico della Fisica e Centro Studi e Ricerche “Enrico Fermi”, Italy; MEXT Grant-in-Aid for Specially Promoted Research, Japan; Joint Institute for Nuclear Research, Dubna; National Research Foundation of Korea (NRF); CONACYT, DGAPA, México, ALFA-EC and the HELEN Program (High-Energy Physics Latin-American-European Network); Stichting voor Fundamenteel Onderzoek der Materie (FOM) and the Nederlandse Organisatie voor Wetenschappelijk Onderzoek (NWO), Netherlands; Research Council of Norway (NFR); Polish Ministry of Science and Higher Education; National Authority for Scientific Research – NASR (Autoritatea Națională pentru Cercetare Științifică – ANCS); Ministry of Education and Science of Russian Federation, International Science and Technology Center, Russian Academy of Sciences, Russian Federal Agency of Atomic Energy, Russian Federal Agency for Science and Innovations and CERN-INTAS; Ministry of Education of Slovakia; Department of Science and Technology, South Africa; CIEMAT, EELA, Ministerio de Educación y Ciencia of Spain, Xunta de Galicia (Consellería de Educación), CEADEN, Cubaenergía, Cuba, and IAEA (International Atomic Energy Agency); Swedish Research Council (VR) and Knut & Alice Wallenberg Foundation (KAW); Ukraine Ministry of Education and Science; United Kingdom Science and Technology Facilities Council (STFC); The United States Department of Energy, the United States National Science Foundation, the State of Texas, and the State of Ohio.

Open access

This article is published Open Access at sciencedirect.com. It is distributed under the terms of the Creative Commons Attribution License 3.0, which permits unrestricted use, distribution, and

reproduction in any medium, provided the original authors and source are credited.

References

- [1] D. Acosta, et al., Phys. Rev. D 71 (2005) 032001.
- [2] M. Cacciari, M. Greco, P. Nason, JHEP 9805 (1998) 007.
- [3] M. Cacciari, S. Frixione, P. Nason, JHEP 0103 (2001) 006.
- [4] D. Acosta, et al., Phys. Rev. Lett. 91 (2003) 241804.
- [5] A. Adare, et al., Phys. Rev. C 84 (2011) 044905.
- [6] L. Adamczyk, et al., Measurements of D^0 and D^* production in $p + p$ collisions at $\sqrt{s} = 200$ GeV, arXiv:1204.4244 [nucl-ex], 2012.
- [7] R. Aaij, et al., JHEP 1204 (2012) 093, and references therein.
- [8] S. Chatrchyan, et al., Phys. Rev. D 84 (2011) 052008, and references therein.
- [9] B. Abelev, et al., JHEP 11 (2012) 065.
- [10] K. Aamodt, et al., JHEP 01 (2012) 128.
- [11] G. Aad, et al., Phys. Lett. B 707 (2012) 438.
- [12] B. Abelev, et al., Phys. Rev. D 86 (2012) 112007, arXiv:1205.5423 [hep-ex].
- [13] B. Abelev, et al., Phys. Lett. B 708 (2012) 265.
- [14] K. Aamodt, et al., JINST 3 (2008) S08002.
- [15] B. Abelev, et al., Measurement of inelastic, single- and double-diffraction cross sections in proton–proton collisions at the LHC with ALICE, arXiv:1208.4968 [hep-ex], 2012.
- [16] P. Billoir, Nucl. Instrum. Meth. 225 (1984) 352.
- [17] R. Brun, et al., CERN program library long write-up, 1994, W5013.
- [18] T. Sjostrand, S. Mrenna, P. Skands, JHEP 0605 (2006) 026.
- [19] P.Z. Skands, The Perugia Tunes, 2009.
- [20] M. Cacciari, S. Frixione, N. Houdeau, M.L. Mangano, P. Nason, et al., JHEP 1210 (2012) 137.
- [21] B. Abelev, et al., Phys. Lett. B 717 (2012) 162.
- [22] B. Abelev, et al., Phys. Lett. B 718 (2012) 279.
- [23] S. Chekanov, et al., Eur. Phys. J. C 44 (2005) 351.
- [24] S. Gorbunov, I. Kisel, Reconstruction of decay particles based on the Kalman filter, private communication, 2007.
- [25] J. Beringer, et al., Phys. Rev. D 86 (2012) 010001.
- [26] P.M. Nadolsky, et al., Phys. Rev. D 78 (2008) 013004.
- [27] L. Lyons, D. Gibaut, P. Clifford, Nucl. Instrum. Meth. A 270 (1988) 110.
- [28] B. Abelev, et al., JHEP 1207 (2012) 191.

ALICE Collaboration

B. Abelev⁶⁸, J. Adam³⁴, D. Adamová⁷³, A.M. Adare¹¹⁸, M.M. Aggarwal⁷⁷, G. Aglieri Rinella³⁰, A.G. Agocs⁶⁰, A. Agostinelli¹⁹, S. Aguilar Salazar⁵⁶, Z. Ahammed¹¹⁴, N. Ahmad¹⁴, A. Ahmad Masoodi¹⁴, S.A. Ahn⁶², S.U. Ahn³⁷, A. Akindinov⁴⁶, D. Aleksandrov⁸⁸, B. Alessandro⁹⁴, R. Alfaro Molina⁵⁶, A. Alici^{97,10}, A. Alkin², E. Almaráz Aviña⁵⁶, J. Alme³², T. Alt³⁶, V. Altini²⁸, S. Altinpinar¹⁵, I. Altsybeev¹¹⁵, C. Andrei⁷⁰, A. Andronic⁸⁵, V. Angelov⁸², J. Anielski⁵⁴, C. Anson¹⁶, T. Antičić⁸⁶, F. Antinori⁹³, P. Antonioli⁹⁷, L. Aphecetche¹⁰¹, H. Appelshäuser⁵², N. Arbor⁶⁴, S. Arcelli¹⁹, A. Arend⁵², N. Armesto¹³, R. Arnaldi⁹⁴, T. Aronsson¹¹⁸, I.C. Arsene⁸⁵, M. Arslandok⁵², A. Asryan¹¹⁵, A. Augustinus³⁰, R. Averbeck⁸⁵, T.C. Awes⁷⁴, J. Äystö³⁸, M.D. Azmi^{14,79}, M. Bach^{36,i}, A. Badalà⁹⁹, Y.W. Baek^{63,37}, R. Bailhache⁵², R. Bala⁹⁴, R. Baldini Ferroli¹⁰, A. Baldisseri¹², A. Baldit⁶³, F. Baltasar Dos Santos Pedrosa³⁰, J. Bán⁴⁷, R.C. Baral⁴⁸, R. Barbera²⁵, F. Barile²⁸, G.G. Barnaföldi⁶⁰, L.S. Barnby⁹⁰, V. Barret⁶³, J. Bartke¹⁰³, M. Basile¹⁹, N. Bastid⁶³, S. Basu¹¹⁴, B. Bathen⁵⁴, G. Batigne¹⁰¹, B. Batyunya⁵⁹, C. Baumann⁵², I.G. Bearden⁷¹, H. Beck⁵², N.K. Behera⁴⁰, I. Belikov⁵⁸, F. Bellini¹⁹, R. Bellwied¹⁰⁹, E. Belmont-Moreno⁵⁶, G. Bencedi⁶⁰, S. Beole²³, I. Berceanu⁷⁰, A. Bercuci⁷⁰, Y. Berdnikov⁷⁵, D. Berenyi⁶⁰, A.A.E. Bergognon¹⁰¹, D. Berzano⁹⁴, L. Betev³⁰, A. Bhasin⁸⁰, A.K. Bhati⁷⁷, J. Bhom¹¹², L. Bianchi²³, N. Bianchi⁶⁵, C. Bianchin²⁰, J. Bielčík³⁴, J. Bielčíková⁷³, A. Bilandzic⁷¹, S. Bjelogrić⁴⁵, F. Blanco⁸, F. Blanco¹⁰⁹, D. Blau⁸⁸, C. Blume⁵², M. Boccioni³⁰, N. Bock¹⁶, S. Böttger⁵¹, A. Bogdanov⁶⁹, H. Bøggild⁷¹, M. Bogolyubsky⁴³, L. Boldizsár⁶⁰, M. Bombara³⁵, J. Book⁵², H. Borel¹², A. Borissov¹¹⁷, S. Bose⁸⁹, F. Bossú^{79,23}, M. Botje⁷², E. Botta²³, B. Boyer⁴², E. Braidot⁶⁷, P. Braun-Munzinger⁸⁵, M. Bregant¹⁰¹, T. Breitner⁵¹, T.A. Browning⁸³, M. Broz³³, R. Brun³⁰, E. Bruna^{23,94}, G.E. Bruno²⁸, D. Budnikov⁸⁷, H. Buesching⁵², S. Bufalino^{23,94}, O. Busch⁸², Z. Buthelezi⁷⁹, D. Caballero Orduna¹¹⁸, D. Caffarri^{20,93}, X. Cai⁵, H. Caines¹¹⁸, E. Calvo Villar⁹¹, P. Camerini²¹, V. Canoa Roman⁹, G. Cara Romeo⁹⁷, F. Carena³⁰, W. Carena³⁰, N. Carlin Filho¹⁰⁶, F. Carminati³⁰, A. Casanova Díaz⁶⁵, J. Castillo Castellanos¹², J.F. Castillo Hernandez⁸⁵, E.A.R. Casula²², V. Catanescu⁷⁰,

C. Cavicchioli³⁰, C. Ceballos Sanchez⁷, J. Cepila³⁴, P. Cerello⁹⁴, B. Chang^{38,121}, S. Chapeland³⁰, J.L. Charvet¹², S. Chattopadhyay¹¹⁴, S. Chattopadhyay⁸⁹, I. Chawla⁷⁷, M. Cherney⁷⁶, C. Cheshkov^{30,108}, B. Cheynis¹⁰⁸, V. Chibante Barroso³⁰, D.D. Chinellato¹⁰⁷, P. Chochula³⁰, M. Chojnacki⁴⁵, S. Choudhury¹¹⁴, P. Christakoglou⁷², C.H. Christensen⁷¹, P. Christiansen²⁹, T. Chujo¹¹², S.U. Chung⁸⁴, C. Cicalo⁹⁶, L. Cifarelli^{19,30,10}, F. Cindolo⁹⁷, J. Cleymans⁷⁹, F. Coccetti¹⁰, F. Colamaria²⁸, D. Colella²⁸, G. Conesa Balbastre⁶⁴, Z. Conesa del Valle³⁰, P. Constantin⁸², G. Contin²¹, J.G. Contreras⁹, T.M. Cormier¹¹⁷, Y. Corrales Morales²³, P. Cortese²⁷, I. Cortés Maldonado¹, M.R. Cosentino⁶⁷, F. Costa³⁰, M.E. Cotallo⁸, E. Crescio⁹, P. Crochet⁶³, E. Cruz Alaniz⁵⁶, E. Cuautle⁵⁵, L. Cunqueiro⁶⁵, A. Dainese^{20,93}, H.H. Dalsgaard⁷¹, A. Danu⁵⁰, D. Das⁸⁹, I. Das⁴², K. Das⁸⁹, A. Dash¹⁰⁷, S. Dash⁴⁰, S. De¹¹⁴, G.O.V. de Barros¹⁰⁶, A. De Caro^{26,10}, G. de Cataldo⁹⁸, J. de Cuveland³⁶, A. De Falco²², D. De Gruttola²⁶, H. Delagrange¹⁰¹, A. Deloff¹⁰⁰, V. Demanov⁸⁷, N. De Marco⁹⁴, E. Dénes⁶⁰, S. De Pasquale²⁶, A. Deppman¹⁰⁶, G. D Erasmo²⁸, R. de Rooij⁴⁵, M.A. Diaz Corchero⁸, D. Di Bari²⁸, T. Dietel⁵⁴, C. Di Giglio²⁸, S. Di Liberto⁹⁵, A. Di Mauro³⁰, P. Di Nezza⁶⁵, R. Divià³⁰, Ø. Djuvsland¹⁵, A. Dobrin^{117,29}, T. Dobrowolski¹⁰⁰, I. Domínguez⁵⁵, B. Dönigus⁸⁵, O. Dordic¹⁸, O. Driga¹⁰¹, A.K. Dubey¹¹⁴, A. Dubla⁴⁵, L. Ducroux¹⁰⁸, P. Dupieux⁶³, M.R. Dutta Majumdar¹¹⁴, A.K. Dutta Majumdar⁸⁹, D. Elia⁹⁸, D. Emschermann⁵⁴, H. Engel⁵¹, B. Erazmus^{30,101}, H.A. Erdal³², B. Espagnon⁴², M. Estienne¹⁰¹, S. Esumi¹¹², D. Evans⁹⁰, G. Eyyubova¹⁸, D. Fabris^{20,93}, J. Faivre⁶⁴, D. Falchieri¹⁹, A. Fantoni⁶⁵, M. Fasel⁸⁵, R. Fearick⁷⁹, A. Fedunov⁵⁹, D. Fehlker¹⁵, L. Feldkamp⁵⁴, D. Felea⁵⁰, B. Fenton-Olsen⁶⁷, G. Feofilov¹¹⁵, A. Fernández Téllez¹, A. Ferretti²³, R. Ferretti²⁷, A. Festanti²⁰, J. Figiel¹⁰³, M.A.S. Figueredo¹⁰⁶, S. Filchagin⁸⁷, D. Finogeev⁴⁴, F.M. Fionda²⁸, E.M. Fiore²⁸, M. Floris³⁰, S. Foertsch⁷⁹, P. Foka⁸⁵, S. Fokin⁸⁸, E. Fragiaco⁹², A. Francescon^{30,20}, U. Frankenfeld⁸⁵, U. Fuchs³⁰, C. Furget⁶⁴, M. Fusco Girard²⁶, J.J. Gaardhøje⁷¹, M. Gagliardi²³, A. Gago⁹¹, M. Gallio²³, D.R. Gangadharan¹⁶, P. Ganoti⁷⁴, C. Garabatos⁸⁵, E. Garcia-Solis¹¹, I. Garishvili⁶⁸, J. Gerhard³⁶, M. Germain¹⁰¹, C. Geuna¹², A. Gheata³⁰, M. Gheata^{50,30}, B. Ghidini²⁸, P. Ghosh¹¹⁴, P. Gianotti⁶⁵, M.R. Girard¹¹⁶, P. Giubellino³⁰, E. Gladysz-Dziadus¹⁰³, P. Glässel⁸², R. Gomez^{105,9}, E.G. Ferreira¹³, L.H. González-Trueba⁵⁶, P. González-Zamora⁸, S. Gorbunov³⁶, A. Goswami⁸¹, S. Gotovac¹⁰², V. Grabski⁵⁶, L.K. Graczykowski¹¹⁶, R. Grajcarek⁸², A. Grelli⁴⁵, C. Grigoras³⁰, A. Grigoras³⁰, V. Grigoriev⁶⁹, A. Grigoryan¹¹⁹, S. Grigoryan⁵⁹, B. Grinyov², N. Grion⁹², P. Gros²⁹, J.F. Grosse-Oetringhaus³⁰, J.-Y. Grossiord¹⁰⁸, R. Grosso³⁰, F. Guber⁴⁴, R. Guernane⁶⁴, C. Guerra Gutierrez⁹¹, B. Guerzoni¹⁹, M. Guilbaud¹⁰⁸, K. Gulbrandsen⁷¹, T. Gunji¹¹¹, A. Gupta⁸⁰, R. Gupta⁸⁰, H. Gutbrod⁸⁵, Ø. Haaland¹⁵, C. Hadjidakis⁴², M. Haiduc⁵⁰, H. Hamagaki¹¹¹, G. Hamar⁶⁰, B.H. Han¹⁷, L.D. Hanratty⁹⁰, A. Hansen⁷¹, Z. Harmanová-Tóthová³⁵, J.W. Harris¹¹⁸, M. Hartig⁵², D. Hasegan⁵⁰, D. Hatzifotiadou⁹⁷, A. Hayrapetyan^{30,119}, S.T. Heckel⁵², M. Heide⁵⁴, H. Helstrup³², A. Herghelegiu⁷⁰, G. Herrera Corral⁹, N. Herrmann⁸², B.A. Hess¹¹³, K.F. Hetland³², B. Hicks¹¹⁸, P.T. Hille¹¹⁸, B. Hippolyte⁵⁸, T. Horaguchi¹¹², Y. Hori¹¹¹, P. Hristov³⁰, I. Hřivnáčová⁴², M. Huang¹⁵, T.J. Humanic¹⁶, D.S. Hwang¹⁷, R. Ichou⁶³, R. Ilkaev⁸⁷, I. Ilkiv¹⁰⁰, M. Inaba¹¹², E. Incani²², P.G. Innocenti³⁰, G.M. Innocenti²³, M. Ippolitov⁸⁸, M. Irfan¹⁴, C. Ivan⁸⁵, V. Ivanov⁷⁵, A. Ivanov¹¹⁵, M. Ivanov⁸⁵, O. Ivanytskyi², P.M. Jacobs⁶⁷, H.J. Jang⁶², M.A. Janik¹¹⁶, R. Janik³³, P.H.S.Y. Jayarathna¹⁰⁹, S. Jena⁴⁰, D.M. Jha¹¹⁷, R.T. Jimenez Bustamante⁵⁵, L. Jirde³⁰, P.G. Jones⁹⁰, H. Jung³⁷, A. Jusko⁹⁰, A.B. Kaidalov⁴⁶, V. Kakoyan¹¹⁹, S. Kalcher³⁶, P. Kaliňák⁴⁷, T. Kalliokoski³⁸, A. Kalweit^{53,30}, J.H. Kang¹²¹, V. Kaplin⁶⁹, A. Karasu Uysal^{30,120}, O. Karavichev⁴⁴, T. Karavicheva⁴⁴, E. Karpechev⁴⁴, A. Kazantsev⁸⁸, U. Kebschull⁵¹, R. Keidel¹²², M.M. Khan¹⁴, S.A. Khan¹¹⁴, P. Khan⁸⁹, A. Khanzadeev⁷⁵, Y. Kharlov⁴³, B. Kileng³², M. Kim¹²¹, D.W. Kim³⁷, J.H. Kim¹⁷, J.S. Kim³⁷, M. Kim³⁷, S. Kim¹⁷, D.J. Kim³⁸, B. Kim¹²¹, T. Kim¹²¹, S. Kirsch³⁶, I. Kisel³⁶, S. Kiselev⁴⁶, A. Kisiel¹¹⁶, J.L. Klay⁴, J. Klein⁸², C. Klein-Bösing⁵⁴, M. Kliemant⁵², A. Kluge³⁰, M.L. Knichel⁸⁵, A.G. Knospe¹⁰⁴, K. Koch⁸², M.K. Köhler⁸⁵, T. Kollegger³⁶, A. Kolojvari¹¹⁵, V. Kondratiev¹¹⁵, N. Kondratyeva⁶⁹, A. Konevskikh⁴⁴, A. Korneev⁸⁷, R. Kour⁹⁰, M. Kowalski¹⁰³, S. Kox⁶⁴, G. Koyithatta Meethalevedu⁴⁰, J. Kral³⁸, I. Králik⁴⁷, F. Kramer⁵², I. Kraus⁸⁵, T. Krawutschke^{82,31}, M. Krelina³⁴, M. Kretz³⁶, M. Krivda^{90,47}, F. Krizek³⁸, M. Krus³⁴, E. Kryshen⁷⁵, M. Krzewicki⁸⁵, Y. Kucheriaev⁸⁸, T. Kugathasan³⁰, C. Kuhn⁵⁸, P.G. Kuijer⁷², I. Kulakov⁵², J. Kumar⁴⁰, P. Kurashvili¹⁰⁰, A. Kurepin⁴⁴, A.B. Kurepin⁴⁴, A. Kuryakin⁸⁷, S. Kushpil⁷³, V. Kushpil⁷³, H. Kvaerno¹⁸, M.J. Kweon^{82,*}, Y. Kwon¹²¹, P. Ladrón de Guevara⁵⁵, I. Lakomov⁴², R. Langoy¹⁵, S.L. La Pointe⁴⁵, C. Lara⁵¹, A. Lardeux¹⁰¹, P. La Rocca²⁵, R. Lea²¹, Y. Le Bornec⁴², M. Lechman³⁰, K.S. Lee³⁷, S.C. Lee³⁷, G.R. Lee⁹⁰, F. Lefèvre¹⁰¹, J. Lehnert⁵², M. Lenhardt⁸⁵, V. Lenti⁹⁸, H. León⁵⁶, M. Leoncino⁹⁴,

I. León Monzón¹⁰⁵, H. León Vargas⁵², P. Lévai⁶⁰, J. Lien¹⁵, R. Lietava⁹⁰, S. Lindal¹⁸, V. Lindenstruth³⁶, C. Lippmann^{85,30}, M.A. Lisa¹⁶, L. Liu¹⁵, V.R. Loggins¹¹⁷, V. Loginov⁶⁹, S. Lohn³⁰, D. Lohner⁸², C. Loizides⁶⁷, K.K. Loo³⁸, X. Lopez⁶³, E. López Torres⁷, G. Løvhøiden¹⁸, X.-G. Lu⁸², P. Luettig⁵², M. Lunardon²⁰, J. Luo⁵, G. Luparello⁴⁵, L. Luquin¹⁰¹, C. Luzzi³⁰, R. Ma¹¹⁸, K. Ma⁵, D.M. Madagodahettige-Don¹⁰⁹, A. Maevskaya⁴⁴, M. Mager^{53,30}, D.P. Mahapatra⁴⁸, A. Maire⁸², M. Malaev⁷⁵, I. Maldonado Cervantes⁵⁵, L. Malinina^{59,i}, D. Mal'Kevich⁴⁶, P. Malzacher⁸⁵, A. Mamonov⁸⁷, L. Mangotra⁸⁰, V. Manko⁸⁸, F. Manso⁶³, V. Manzari⁹⁸, Y. Mao⁵, M. Marchisone^{63,23}, J. Mareš⁴⁹, G.V. Margagliotti^{21,92}, A. Margotti⁹⁷, A. Marín⁸⁵, C.A. Marin Tobon³⁰, C. Markert¹⁰⁴, I. Martashvili¹¹⁰, P. Martinengo³⁰, M.I. Martínez¹, A. Martínez Davalos⁵⁶, G. Martínez García¹⁰¹, Y. Martynov², A. Mas¹⁰¹, S. Masciocchi⁸⁵, M. Maserà²³, A. Masoni⁹⁶, L. Massacrier¹⁰¹, A. Mastroserio²⁸, Z.L. Matthews⁹⁰, A. Matyja^{103,101}, C. Mayer¹⁰³, J. Mazer¹¹⁰, M.A. Mazzoni⁹⁵, F. Meddi²⁴, A. Menchaca-Rocha⁵⁶, J. Mercado Pérez⁸², M. Meres³³, Y. Miake¹¹², L. Milano²³, J. Milosevic^{18,ii}, A. Mischke⁴⁵, A.N. Mishra⁸¹, D. Miśkowiec^{85,30}, C. Mitu⁵⁰, J. Mlynarz¹¹⁷, B. Mohanty¹¹⁴, L. Molnar^{60,30}, L. Montaño Zetina⁹, M. Monteno⁹⁴, E. Montes⁸, T. Moon¹²¹, M. Morando²⁰, D.A. Moreira De Godoy¹⁰⁶, S. Moretto²⁰, A. Morsch³⁰, V. Muccifora⁶⁵, E. Mudnic¹⁰², S. Muhuri¹¹⁴, M. Mukherjee¹¹⁴, H. Müller³⁰, M.G. Munhoz¹⁰⁶, L. Musa³⁰, A. Musso⁹⁴, B.K. Nandi⁴⁰, R. Nania⁹⁷, E. Nappi⁹⁸, C. Nattrass¹¹⁰, N.P. Naumov⁸⁷, S. Navin⁹⁰, T.K. Nayak¹¹⁴, S. Nazarenko⁸⁷, G. Nazarov⁸⁷, A. Nedosekin⁴⁶, M. Nicassio²⁸, M. Niculescu^{50,30}, B.S. Nielsen⁷¹, T. Niida¹¹², S. Nikolaev⁸⁸, V. Nikolic⁸⁶, S. Nikulin⁸⁸, V. Nikulin⁷⁵, B.S. Nilsen⁷⁶, M.S. Nilsson¹⁸, F. Noferini^{97,10}, P. Nomokonov⁵⁹, G. Nooren⁴⁵, N. Novitzky³⁸, A. Nyanin⁸⁸, A. Nyatha⁴⁰, C. Nygaard⁷¹, J. Nystrand¹⁵, A. Ochirov¹¹⁵, H. Oeschler^{53,30}, S. Oh¹¹⁸, S.K. Oh³⁷, J. Oleniacz¹¹⁶, C. Oppedisano⁹⁴, A. Ortiz Velasquez^{29,55}, G. Ortona²³, A. Oskarsson²⁹, P. Ostrowski¹¹⁶, J. Otwinowski⁸⁵, K. Oyama⁸², K. Ozawa¹¹¹, Y. Pachmayer⁸², M. Pachr³⁴, F. Padilla²³, P. Pagano²⁶, G. Paić⁵⁵, F. Painke³⁶, C. Pajares¹³, S.K. Pal¹¹⁴, A. Palaha⁹⁰, A. Palmeri⁹⁹, V. Papikyan¹¹⁹, G.S. Pappalardo⁹⁹, W.J. Park⁸⁵, A. Passfeld⁵⁴, B. Pastirčák⁴⁷, D.I. Patalakha⁴³, V. Patricchio⁹⁸, A. Pavlinov¹¹⁷, T. Pawlak¹¹⁶, T. Peitzmann⁴⁵, H. Pereira Da Costa¹², E. Pereira De Oliveira Filho¹⁰⁶, D. Peresunko⁸⁸, C.E. Pérez Lara⁷², E. Perez Lezama⁵⁵, D. Perini³⁰, D. Perrino²⁸, W. Peryt¹¹⁶, A. Pesci⁹⁷, V. Peskov^{30,55}, Y. Pestov³, V. Petráček³⁴, M. Petran³⁴, M. Petris⁷⁰, P. Petrov⁹⁰, M. Petrovici⁷⁰, C. Petta²⁵, S. Piano⁹², A. Piccotti⁹⁴, M. Pikna³³, P. Pillot¹⁰¹, O. Pinazza³⁰, L. Pinsky¹⁰⁹, N. Pitz⁵², D.B. Piyarathna¹⁰⁹, M. Planinic⁸⁶, M. Płoskoń⁶⁷, J. Pluta¹¹⁶, T. Pocheptsov⁵⁹, S. Pochybova⁶⁰, P.L.M. Podesta-Lerma¹⁰⁵, M.G. Poghosyan^{30,23}, K. Polák⁴⁹, B. Polichtchouk⁴³, A. Pop⁷⁰, S. Porteboeuf-Houssais⁶³, V. Pospíšil³⁴, B. Potukuchi⁸⁰, S.K. Prasad¹¹⁷, R. Preghenella^{97,10}, F. Prino⁹⁴, C.A. Pruneau¹¹⁷, I. Pshenichnov⁴⁴, S. Puchagin⁸⁷, G. Puddu²², A. Pulvirenti²⁵, V. Punin⁸⁷, M. Putiš³⁵, J. Putschke^{117,118}, E. Quercigh³⁰, H. Qvigstad¹⁸, A. Rachevski⁹², A. Rademakers³⁰, T.S. Rähä³⁸, J. Rak³⁸, A. Rakotozafindrabe¹², L. Ramello²⁷, A. Ramírez Reyes⁹, R. Raniwala⁸¹, S. Raniwala⁸¹, S.S. Räsänen³⁸, B.T. Rascanu⁵², D. Rathee⁷⁷, K.F. Read¹¹⁰, J.S. Real⁶⁴, K. Redlich^{100,57}, P. Reichelt⁵², M. Reicher⁴⁵, R. Renfordt⁵², A.R. Reolon⁶⁵, A. Reshetin⁴⁴, F. Rettig³⁶, J.-P. Revol³⁰, K. Reygers⁸², L. Riccati⁹⁴, R.A. Ricci⁶⁶, T. Richert²⁹, M. Richter¹⁸, P. Riedler³⁰, W. Riegler³⁰, F. Riggi^{25,99}, B. Rodrigues Fernandes Rabacal³⁰, M. Rodríguez Cahuantzi¹, A. Rodriguez Manso⁷², K. Røed¹⁵, D. Rohr³⁶, D. Röhrich¹⁵, R. Romita⁸⁵, F. Ronchetti⁶⁵, P. Rosnet⁶³, S. Rossegger³⁰, A. Rossi^{30,20}, C. Roy⁵⁸, P. Roy⁸⁹, A.J. Rubio Montero⁸, R. Rui²¹, R. Russo²³, E. Ryabinkin⁸⁸, A. Rybicki¹⁰³, S. Sadovsky⁴³, K. Šafařík³⁰, R. Sahoo⁴¹, P.K. Sahu⁴⁸, J. Saini¹¹⁴, H. Sakaguchi³⁹, S. Sakai⁶⁷, D. Sakata¹¹², C.A. Salgado¹³, J. Salzwedel¹⁶, S. Sambyal⁸⁰, V. Samsonov⁷⁵, X. Sanchez Castro⁵⁸, L. Šándor⁴⁷, A. Sandoval⁵⁶, S. Sano¹¹¹, M. Sano¹¹², R. Santo⁵⁴, R. Santoro^{98,30,10}, J. Sarkamo³⁸, E. Scapparone⁹⁷, F. Scarlassara²⁰, R.P. Scharenberg⁸³, C. Schiaua⁷⁰, R. Schicker⁸², C. Schmidt⁸⁵, H.R. Schmidt¹¹³, S. Schreiner³⁰, S. Schuchmann⁵², J. Schukraft³⁰, Y. Schutz^{30,101}, K. Schwarz⁸⁵, K. Schweda^{85,82}, G. Scioli¹⁹, E. Scomparin⁹⁴, R. Scott¹¹⁰, G. Segato²⁰, I. Selyuzhenkov⁸⁵, S. Senyukov⁵⁸, J. Seo⁸⁴, S. Serci²², E. Serradilla^{8,56}, A. Sevcenco⁵⁰, A. Shabetai¹⁰¹, G. Shabratova⁵⁹, R. Shahoyan³⁰, S. Sharma⁸⁰, N. Sharma⁷⁷, S. Rohni⁸⁰, K. Shigaki³⁹, M. Shimomura¹¹², K. Shtejer⁷, Y. Sibiriyak⁸⁸, M. Siciliano²³, E. Sickling³⁰, S. Siddhanta⁹⁶, T. Siemiarczuk¹⁰⁰, D. Silvermyr⁷⁴, C. Silvestre⁶⁴, G. Simatovic^{55,86}, G. Simonetti³⁰, R. Singaraju¹¹⁴, R. Singh⁸⁰, S. Singha¹¹⁴, V. Singhal¹¹⁴, B.C. Sinha¹¹⁴, T. Sinha⁸⁹, B. Sitar³³, M. Sitta²⁷, T.B. Skaali¹⁸, K. Skjerdal¹⁵, R. Smakal³⁴, N. Smirnov¹¹⁸, R.J.M. Snellings⁴⁵, C. Søgaard⁷¹, R. Soltz⁶⁸, H. Son¹⁷, J. Song⁸⁴, M. Song¹²¹, C. Soos³⁰, F. Soramel²⁰,

I. Sputowska¹⁰³, M. Spyropoulou-Stassinaki⁷⁸, B.K. Srivastava⁸³, J. Stachel⁸², I. Stan⁵⁰, I. Stan⁵⁰, G. Stefanek¹⁰⁰, M. Steinpreis¹⁶, E. Stenlund²⁹, G. Steyn⁷⁹, J.H. Stiller⁸², D. Stocco¹⁰¹, M. Stolpovskiy⁴³, K. Strabykin⁸⁷, P. Strmen³³, A.A.P. Suaide¹⁰⁶, M.A. Subieta Vásquez²³, T. Sugitate³⁹, C. Suire⁴², M. Sukhorukov⁸⁷, R. Sultanov⁴⁶, M. Šumbera⁷³, T. Susa⁸⁶, T.J.M. Symons⁶⁷, A. Szanto de Toledo¹⁰⁶, I. Szarka³³, A. Szczepankiewicz^{103,30}, A. Szostak¹⁵, M. Szymański¹¹⁶, J. Takahashi¹⁰⁷, J.D. Tapia Takaki⁴², A. Tauro³⁰, G. Tejeda Muñoz¹, A. Telesca³⁰, C. Terrevoli²⁸, J. Thäder⁸⁵, D. Thomas⁴⁵, R. Tieulent¹⁰⁸, A.R. Timmins¹⁰⁹, D. Tlusty³⁴, A. Toia^{36,20,93}, H. Torii¹¹¹, L. Toscano⁹⁴, V. Trubnikov², D. Truesdale¹⁶, W.H. Trzaska³⁸, T. Tsuji¹¹¹, A. Tumkin⁸⁷, R. Turrisi⁹³, T.S. Tveter¹⁸, J. Ulery⁵², K. Ullaland¹⁵, J. Ulrich^{61,51}, A. Uras¹⁰⁸, J. Urbán³⁵, G.M. Urciuoli⁹⁵, G.L. Usai²², M. Vajzer^{34,73}, M. Vala^{59,47}, L. Valencia Palomo⁴², S. Vallero⁸², P. Vande Vyvre³⁰, M. van Leeuwen⁴⁵, L. Vannucci⁶⁶, A. Vargas¹, R. Varma⁴⁰, M. Vasileiou⁷⁸, A. Vasiliev⁸⁸, V. Vechernin¹¹⁵, M. Veldhoen⁴⁵, M. Venaruzzo²¹, E. Vercellin²³, S. Vergara¹, R. Vernet⁶, M. Verweij⁴⁵, L. Vickovic¹⁰², G. Viesti²⁰, O. Vikhlyantsev⁸⁷, Z. Vilakazi⁷⁹, O. Villalobos Baillie⁹⁰, Y. Vinogradov⁸⁷, L. Vinogradov¹¹⁵, A. Vinogradov⁸⁸, T. Virgili²⁶, Y.P. Viyogi¹¹⁴, A. Vodopyanov⁵⁹, K. Voloshin⁴⁶, S. Voloshin¹¹⁷, G. Volpe^{28,30}, B. von Haller³⁰, D. Vranic⁸⁵, G. Øvrebek¹⁵, J. Vrláková³⁵, B. Vulpescu⁶³, A. Vyushin⁸⁷, V. Wagner³⁴, B. Wagner¹⁵, R. Wan⁵, D. Wang⁵, M. Wang⁵, Y. Wang⁵, Y. Wang⁸², K. Watanabe¹¹², M. Weber¹⁰⁹, J.P. Wessels^{30,54}, U. Westerhoff⁵⁴, J. Wiechula¹¹³, J. Wikne¹⁸, M. Wilde⁵⁴, A. Wilk⁵⁴, G. Wilk¹⁰⁰, M.C.S. Williams⁹⁷, B. Windelband⁸², L. Xaplanteris Karampatsos¹⁰⁴, C.G. Yaldo¹¹⁷, Y. Yamaguchi¹¹¹, S. Yang¹⁵, H. Yang¹², S. Yasnopolskiy⁸⁸, J. Yi⁸⁴, Z. Yin⁵, I.-K. Yoo⁸⁴, J. Yoon¹²¹, W. Yu⁵², X. Yuan⁵, I. Yushmanov⁸⁸, V. Zaccaro⁷¹, C. Zach³⁴, C. Zampolli⁹⁷, S. Zaporozhets⁵⁹, A. Zarochentsev¹¹⁵, P. Závada⁴⁹, N. Zaviyalov⁸⁷, H. Zbroszczyk¹¹⁶, P. Zelniczek⁵¹, I.S. Zgura⁵⁰, M. Zhalov⁷⁵, X. Zhang^{63,5}, H. Zhang⁵, F. Zhou⁵, Y. Zhou⁴⁵, D. Zhou⁵, J. Zhu⁵, X. Zhu⁵, J. Zhu⁵, A. Zichichi^{19,10}, A. Zimmermann⁸², G. Zinovjev², Y. Zoccarato¹⁰⁸, M. Zynovyev², M. Zyzak⁵²

¹ Benemérita Universidad Autónoma de Puebla, Puebla, Mexico

² Bogolyubov Institute for Theoretical Physics, Kiev, Ukraine

³ Budker Institute for Nuclear Physics, Novosibirsk, Russia

⁴ California Polytechnic State University, San Luis Obispo, CA, United States

⁵ Central China Normal University, Wuhan, China

⁶ Centre de Calcul de l'IN2P3, Villeurbanne, France

⁷ Centro de Aplicaciones Tecnológicas y Desarrollo Nuclear (CEADEN), Havana, Cuba

⁸ Centro de Investigaciones Energéticas Medioambientales y Tecnológicas (CIEMAT), Madrid, Spain

⁹ Centro de Investigación y de Estudios Avanzados (CINVESTAV), Mexico City and Mérida, Mexico

¹⁰ Centro Fermi – Centro Studi e Ricerche e Museo Storico della Fisica "Enrico Fermi", Rome, Italy

¹¹ Chicago State University, Chicago, United States

¹² Commissariat à l'Energie Atomique, IRFU, Saclay, France

¹³ Departamento de Física de Partículas and IGFAE, Universidad de Santiago de Compostela, Santiago de Compostela, Spain

¹⁴ Department of Physics Aligarh Muslim University, Aligarh, India

¹⁵ Department of Physics and Technology, University of Bergen, Bergen, Norway

¹⁶ Department of Physics, Ohio State University, Columbus, OH, United States

¹⁷ Department of Physics, Sejong University, Seoul, South Korea

¹⁸ Department of Physics, University of Oslo, Oslo, Norway

¹⁹ Dipartimento di Fisica dell'Università and Sezione INFN, Bologna, Italy

²⁰ Dipartimento di Fisica dell'Università and Sezione INFN, Padova, Italy

²¹ Dipartimento di Fisica dell'Università and Sezione INFN, Trieste, Italy

²² Dipartimento di Fisica dell'Università and Sezione INFN, Cagliari, Italy

²³ Dipartimento di Fisica dell'Università and Sezione INFN, Turin, Italy

²⁴ Dipartimento di Fisica dell'Università 'La Sapienza' and Sezione INFN, Rome, Italy

²⁵ Dipartimento di Fisica e Astronomia dell'Università and Sezione INFN, Catania, Italy

²⁶ Dipartimento di Fisica 'E.R. Caianiello' dell'Università and Gruppo Collegato INFN, Salerno, Italy

²⁷ Dipartimento di Scienze e Innovazione Tecnologica dell'Università del Piemonte Orientale and Gruppo Collegato INFN, Alessandria, Italy

²⁸ Dipartimento Interateneo di Fisica 'M. Merlin' and Sezione INFN, Bari, Italy

²⁹ Division of Experimental High Energy Physics, University of Lund, Lund, Sweden

³⁰ European Organization for Nuclear Research (CERN), Geneva, Switzerland

³¹ Fachhochschule Köln, Köln, Germany

³² Faculty of Engineering, Bergen University College, Bergen, Norway

³³ Faculty of Mathematics, Physics and Informatics, Comenius University, Bratislava, Slovakia

³⁴ Faculty of Nuclear Sciences and Physical Engineering, Czech Technical University in Prague, Prague, Czech Republic

³⁵ Faculty of Science, P.J. Šafárik University, Košice, Slovakia

³⁶ Frankfurt Institute for Advanced Studies, Johann Wolfgang Goethe-Universität Frankfurt, Frankfurt, Germany

³⁷ Gangneung-Wonju National University, Gangneung, South Korea

³⁸ Helsinki Institute of Physics (HIP) and University of Jyväskylä, Jyväskylä, Finland

³⁹ Hiroshima University, Hiroshima, Japan

⁴⁰ Indian Institute of Technology Bombay (IIT), Mumbai, India

⁴¹ Indian Institute of Technology Indore (IIT), Indore, India

⁴² Institut de Physique Nucléaire d'Orsay (IPNO), Université Paris-Sud, CNRS-IN2P3, Orsay, France

⁴³ Institute for High Energy Physics, Protvino, Russia

- 44 Institute for Nuclear Research, Academy of Sciences, Moscow, Russia
- 45 Nikhef, National Institute for Subatomic Physics and Institute for Subatomic Physics of Utrecht University, Utrecht, Netherlands
- 46 Institute for Theoretical and Experimental Physics, Moscow, Russia
- 47 Institute of Experimental Physics, Slovak Academy of Sciences, Košice, Slovakia
- 48 Institute of Physics, Bhubaneswar, India
- 49 Institute of Physics, Academy of Sciences of the Czech Republic, Prague, Czech Republic
- 50 Institute of Space Sciences (ISS), Bucharest, Romania
- 51 Institut für Informatik, Johann Wolfgang Goethe-Universität Frankfurt, Frankfurt, Germany
- 52 Institut für Kernphysik, Johann Wolfgang Goethe-Universität Frankfurt, Frankfurt, Germany
- 53 Institut für Kernphysik, Technische Universität Darmstadt, Darmstadt, Germany
- 54 Institut für Kernphysik, Westfälische Wilhelms-Universität Münster, Münster, Germany
- 55 Instituto de Ciencias Nucleares, Universidad Nacional Autónoma de México, Mexico City, Mexico
- 56 Instituto de Física, Universidad Nacional Autónoma de México, Mexico City, Mexico
- 57 Institut of Theoretical Physics, University of Wrocław, Poland
- 58 Institut Pluridisciplinaire Hubert Curien (IPHC), Université de Strasbourg, CNRS-IN2P3, Strasbourg, France
- 59 Joint Institute for Nuclear Research (JINR), Dubna, Russia
- 60 KFKI Research Institute for Particle and Nuclear Physics, Hungarian Academy of Sciences, Budapest, Hungary
- 61 Kirchhoff-Institut für Physik, Ruprecht-Karls-Universität Heidelberg, Heidelberg, Germany
- 62 Korea Institute of Science and Technology Information, Daejeon, South Korea
- 63 Laboratoire de Physique Corpusculaire (LPC), Clermont Université, Université Blaise Pascal, CNRS-IN2P3, Clermont-Ferrand, France
- 64 Laboratoire de Physique Subatomique et de Cosmologie (LPSC), Université Joseph Fourier, CNRS-IN2P3, Institut Polytechnique de Grenoble, Grenoble, France
- 65 Laboratori Nazionali di Frascati, INFN, Frascati, Italy
- 66 Laboratori Nazionali di Legnaro, INFN, Legnaro, Italy
- 67 Lawrence Berkeley National Laboratory, Berkeley, CA, United States
- 68 Lawrence Livermore National Laboratory, Livermore, CA, United States
- 69 Moscow Engineering Physics Institute, Moscow, Russia
- 70 National Institute for Physics and Nuclear Engineering, Bucharest, Romania
- 71 Niels Bohr Institute, University of Copenhagen, Copenhagen, Denmark
- 72 Nikhef, National Institute for Subatomic Physics, Amsterdam, Netherlands
- 73 Nuclear Physics Institute, Academy of Sciences of the Czech Republic, Řež u Prahy, Czech Republic
- 74 Oak Ridge National Laboratory, Oak Ridge, TN, United States
- 75 Petersburg Nuclear Physics Institute, Gatchina, Russia
- 76 Physics Department, Creighton University, Omaha, NE, United States
- 77 Physics Department, Panjab University, Chandigarh, India
- 78 Physics Department, University of Athens, Athens, Greece
- 79 Physics Department, University of Cape Town, iThemba LABS, Cape Town, South Africa
- 80 Physics Department, University of Jammu, Jammu, India
- 81 Physics Department, University of Rajasthan, Jaipur, India
- 82 Physikalisches Institut, Ruprecht-Karls-Universität Heidelberg, Heidelberg, Germany
- 83 Purdue University, West Lafayette, IN, United States
- 84 Pusan National University, Pusan, South Korea
- 85 Research Division and ExtreMe Matter Institute EMMI, GSI Helmholtzzentrum für Schwerionenforschung, Darmstadt, Germany
- 86 Rudjer Bošković Institute, Zagreb, Croatia
- 87 Russian Federal Nuclear Center (VNIIEF), Sarov, Russia
- 88 Russian Research Centre Kurchatov Institute, Moscow, Russia
- 89 Saha Institute of Nuclear Physics, Kolkata, India
- 90 School of Physics and Astronomy, University of Birmingham, Birmingham, United Kingdom
- 91 Sección Física, Departamento de Ciencias, Pontificia Universidad Católica del Perú, Lima, Peru
- 92 Sezione INFN, Trieste, Italy
- 93 Sezione INFN, Padova, Italy
- 94 Sezione INFN, Turin, Italy
- 95 Sezione INFN, Rome, Italy
- 96 Sezione INFN, Cagliari, Italy
- 97 Sezione INFN, Bologna, Italy
- 98 Sezione INFN, Bari, Italy
- 99 Sezione INFN, Catania, Italy
- 100 Soltan Institute for Nuclear Studies, Warsaw, Poland
- 101 SUBATECH, Ecole des Mines de Nantes, Université de Nantes, CNRS-IN2P3, Nantes, France
- 102 Technical University of Split FESB, Split, Croatia
- 103 The Henryk Niewodniczanski Institute of Nuclear Physics, Polish Academy of Sciences, Cracow, Poland
- 104 The University of Texas at Austin, Physics Department, Austin, TX, United States
- 105 Universidad Autónoma de Sinaloa, Culiacán, Mexico
- 106 Universidade de São Paulo (USP), São Paulo, Brazil
- 107 Universidade Estadual de Campinas (UNICAMP), Campinas, Brazil
- 108 Université de Lyon, Université Lyon 1, CNRS/IN2P3, IPN-Lyon, Villeurbanne, France
- 109 University of Houston, Houston, TX, United States
- 110 University of Tennessee, Knoxville, TN, United States
- 111 University of Tokyo, Tokyo, Japan
- 112 University of Tsukuba, Tsukuba, Japan
- 113 Eberhard Karls Universität Tübingen, Tübingen, Germany
- 114 Variable Energy Cyclotron Centre, Kolkata, India
- 115 V. Fock Institute for Physics, St. Petersburg State University, St. Petersburg, Russia
- 116 Warsaw University of Technology, Warsaw, Poland
- 117 Wayne State University, Detroit, MI, United States
- 118 Yale University, New Haven, CT, United States
- 119 Yerevan Physics Institute, Yerevan, Armenia
- 120 Yildiz Technical University, Istanbul, Turkey
- 121 Yonsei University, Seoul, South Korea
- 122 Zentrum für Technologietransfer und Telekommunikation (ZTT), Fachhochschule Worms, Worms, Germany

* Corresponding author.

E-mail address: minjung@physi.uni-heidelberg.de (M.J. Kweon).

ⁱ Also at: M.V. Lomonosov Moscow State University, D.V. Skobeltsyn Institute of Nuclear Physics, Moscow, Russia.

ⁱⁱ Also at University of Belgrade, Faculty of Physics and “Vinča” Institute of Nuclear Sciences, Belgrade, Serbia.

Update

Physics Letters B

Volume 763, Issue , 10 December 2016, Page 507–509

DOI: <https://doi.org/10.1016/j.physletb.2016.10.004>



Corrigendum

Corrigendum to “Measurement of electrons from beauty hadron decays in pp collisions at $\sqrt{s} = 7$ TeV” [Phys. Lett. B 721 (1–3) (2013) 13–23] and “Beauty production in pp collisions at $\sqrt{s} = 2.76$ TeV measured via semi-electronic decays” [Phys. Lett. B 738 (2014) 97–108]



ALICE Collaboration

ARTICLE INFO

Article history:

Available online 25 October 2016

We have identified a bias in the measurement of electrons from beauty-hadron decays in pp collisions at center-of-mass energies $\sqrt{s} = 2.76$ TeV [1] and $\sqrt{s} = 7$ TeV [2]. The efficiency corrections were evaluated using a Monte Carlo simulation, based on PYTHIA as described in [1,2]. When calculating the impact parameter (d_0) cut efficiency for the charm-hadron decay electrons, we did not consider the difference between the impact parameter distributions using the measured D-meson p_T distribution and the one from Monte Carlo.

For weakly decaying hadrons with sufficiently high transverse momentum (p_T), the impact parameter distribution of the daughter particle at a given p_T depends very weakly on the transverse momentum of the mother hadrons. However, at low momentum the impact parameter distribution of the decay particles depends on the momentum distribution of the mother hadrons. Due to the harder p_T spectra of charm hadrons in the Monte Carlo simulation [1,2] compared to the measured ones [3,4], the d_0 cut efficiency of decay electrons was biased towards larger values. Since the background was subtracted from the raw inclusive electron yield after applying the d_0 cut, the charm-hadron decay background was over-estimated.

We have now computed the d_0 distribution of electrons from charm-hadron decays using a Monte Carlo and weighting each electron by the ratio $(dN/dp_T)^{\text{measured}}/(dN/dp_T)^{\text{MC}}$. $(dN/dp_T)^{\text{measured}}$ and $(dN/dp_T)^{\text{MC}}$ are the production yields evaluated at the p_T of the mother charm-hadron of the electron, as obtained from data [3,4] and in the Monte Carlo simulations [1,2], respectively. In such a way, the measured mother p_T spectra are propagated to the impact parameter cut efficiency calculation for the daughter electrons.

Table 1

Effect of the corrected treatment of the D-meson p_T distribution on the d_0 cut efficiency for electrons from charm-hadron decays (ϵ_{d_0}) and the resulting yield of signal electrons (dN^{signal}/dp_T).

7 TeV pp collisions			
p_T interval (GeV/c)	1–2	2–3	3–8
$\epsilon_{d_0}^{\text{updated}}/\epsilon_{d_0}^{\text{previous}}$	0.56–0.60	0.60–0.70	0.70–0.85
$(dN^{\text{signal}}/dp_T)^{\text{updated}}/(dN^{\text{signal}}/dp_T)^{\text{previous}}$	1.6–1.4	1.3–1.2	< 1.1
2.76 TeV pp collisions			
p_T interval (GeV/c)	1–2	2–3	3–8
$\epsilon_{d_0}^{\text{updated}}/\epsilon_{d_0}^{\text{previous}}$	0.74–0.77	0.77–0.85	0.85–0.94
$(dN^{\text{signal}}/dp_T)^{\text{updated}}/(dN^{\text{signal}}/dp_T)^{\text{previous}}$	1.4–1.3	1.2–1.1	< 1.1

The new value of the d_0 cut efficiency ($\epsilon_{d_0}^{\text{updated}}$) of electrons from charm-hadron decays is significantly smaller than that previously evaluated ($\epsilon_{d_0}^{\text{previous}}$) as summarized in Table 1.

In Fig. 1, the raw electron yield, as well as the non-beauty electron background yield, which is subtracted in the analysis, are shown after the application of the track selection criteria. Compared to Fig. 3 in [2], the yield of electrons from charm-hadron decays is smaller by the factor $\epsilon_{d_0}^{\text{updated}}/\epsilon_{d_0}^{\text{previous}}$ given in Table 1. The corresponding yield of beauty-signal electrons (dN^{signal}/dp_T) increases as listed in Table 1. For pp collisions at $\sqrt{s} = 2.76$ TeV, where a similar bias was present, the same procedure has been applied and the correct distributions are shown in Fig. 2 (to be compared with Fig. 2 in [1]). Numerical values of the implication for the d_0 cut efficiency are given in Table 1.

The uncertainty on the d_0 efficiency was evaluated by propagating the statistical and systematic uncertainties of the charm-hadron p_T distributions in [3] to the measurements discussed in this corrigendum. The uncertainty was added in quadrature as an independent contribution to the total systematic uncertainty.

DOIs of original articles: <http://dx.doi.org/10.1016/j.physletb.2013.01.069>,
<http://dx.doi.org/10.1016/j.physletb.2014.09.026>.

<http://dx.doi.org/10.1016/j.physletb.2016.10.004>
 0370-2693

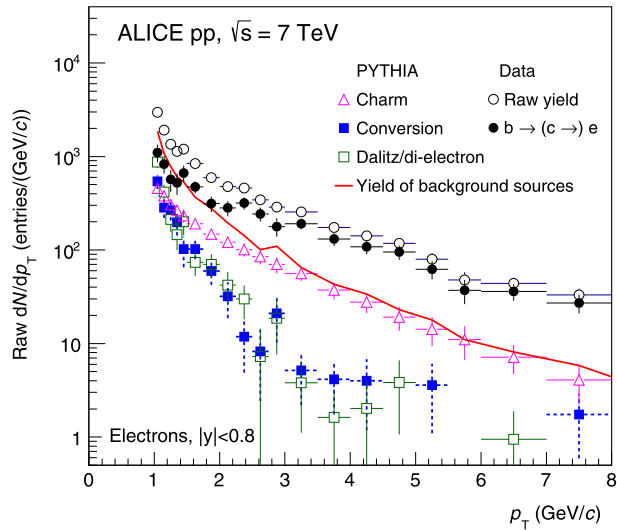


Fig. 1. This figure replaces Fig. 3 from [2]. Caption is the same as Fig. 3 from [2].

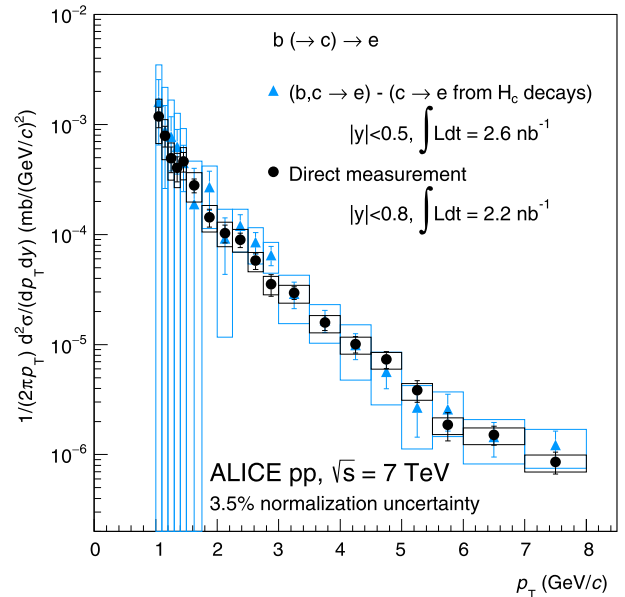


Fig. 3. This figure replaces Fig. 4 from [2]. Caption is the same as Fig. 4 from [2].

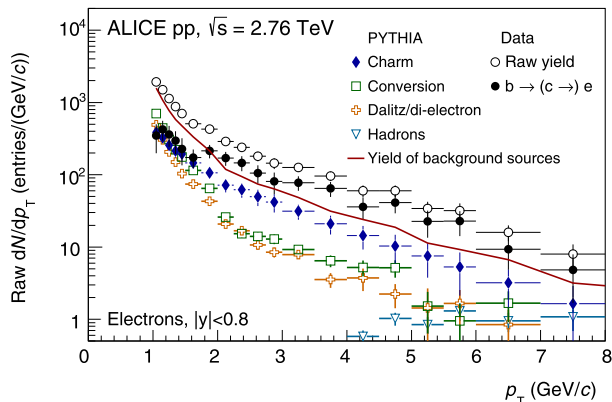


Fig. 2. This figure replaces Fig. 2 from [1]. Caption is the same as Fig. 2 from [1].

Table 2
Summary of the updated cross sections.

Cross sections at 7 TeV pp collisions			
Visible $\sigma_{b \rightarrow e}$	9.03 ± 0.50 (stat)	$^{+2.72}_{-2.73}$ (sys)	± 0.32 (norm) μb
$d\sigma_{b\bar{b}}/dy$	57.7 ± 3.2 (stat)	$^{+17.4}_{-17.4}$ (sys)	$^{+1.4}_{-2.3}$ (extr) ± 2.0 (norm) μb
$\sigma_{b\bar{b}}$	383 ± 21 (stat)	$^{+116}_{-116}$ (sys)	$^{+10}_{-11}$ (extr) ± 13 (norm) ± 13 (br) μb
Weighted $\sigma_{b\bar{b}}$	322 ± 45 (stat)	$^{+58}_{-62}$ (sys)	$^{+8}_{-9}$ (extr) μb
$d\sigma_{c\bar{c}}/dy$	1.1 ± 0.2 (stat)	$^{+0.6}_{-0.7}$ (sys)	$^{+0.2}_{-0.1}$ (extr) mb
$\sigma_{c\bar{c}}$	9.7 ± 1.7 (stat)	$^{+5.2}_{-5.6}$ (sys)	$^{+3.4}_{-0.5}$ (extr) ± 0.4 (br) mb
Cross sections at 2.76 TeV pp collisions			
Visible $\sigma_{b \rightarrow e}$	4.33 ± 0.38 (stat)	$^{+1.45}_{-1.75}$ (sys)	± 0.08 (norm) μb
$d\sigma_{b\bar{b}}/dy$	29.1 ± 2.6 (stat)	$^{+9.8}_{-11.7}$ (sys)	$^{+0.6}_{-0.8}$ (extr) ± 0.6 (norm) μb
$\sigma_{b\bar{b}}$	162 ± 14 (stat)	$^{+55}_{-65}$ (sys)	$^{+4}_{-4}$ (extr) ± 3 (norm) ± 6 (br) μb

The relative systematic uncertainties on the charm-hadron decay background increase by 3% (2%) at $p_T < 1.5$ GeV/c for 7 TeV (2.76 TeV) pp collisions. The change of the systematic uncertainties at higher p_T region is instead negligible. However, the amount of background decreases and as a consequence the total uncertainty on the beauty production measurement decreases.

The production cross sections were also corrected correspondingly. The integrated cross section of electrons from beauty hadron

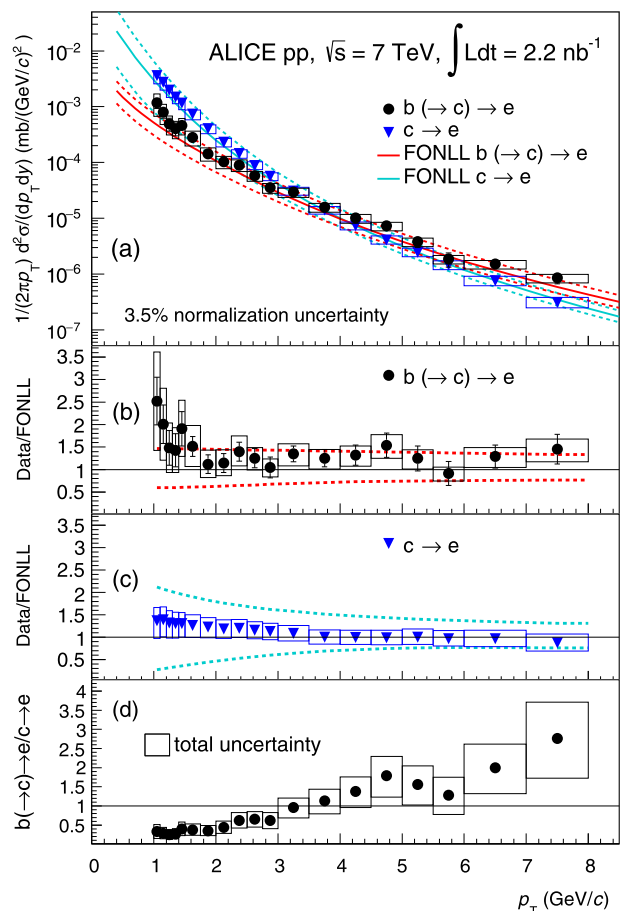


Fig. 4. This figure replaces Fig. 5 from [2]. Caption is the same as Fig. 5 from [2].

decays (visible $\sigma_{b \rightarrow e}$), the beauty production cross section per unit rapidity at mid-rapidity ($d\sigma_{b\bar{b}}/dy$) and the total cross section ($\sigma_{b\bar{b}}$) are summarized in Table 2. For 7 TeV pp collisions, the weighted average of this with the result of a previous measurement of

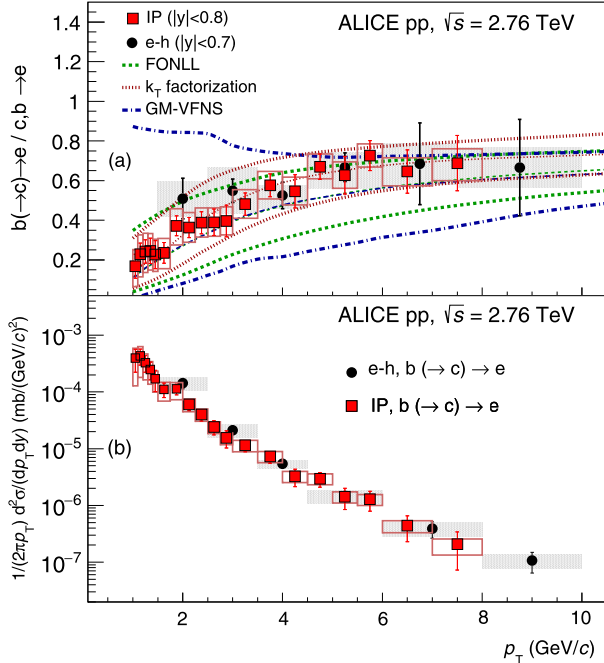


Fig. 5. This figure replaces Fig. 4 from [1]. Caption is the same as Fig. 4 from [1].

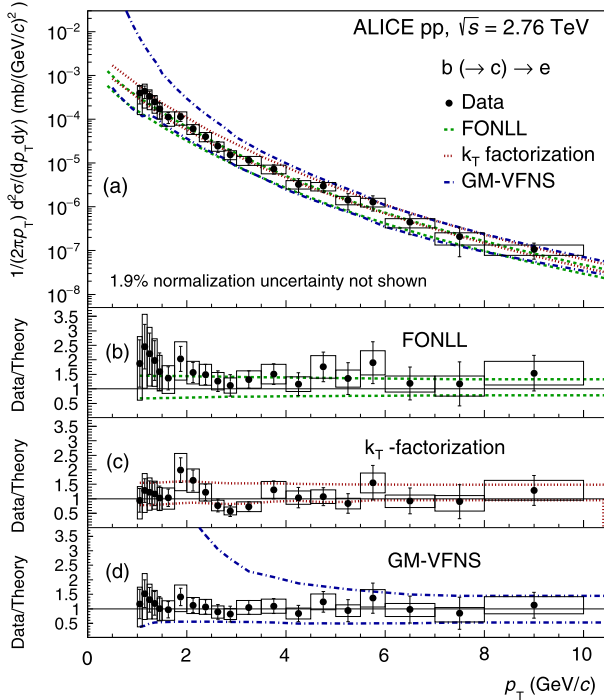


Fig. 6. This figure replaces Fig. 5 from [1]. Caption is the same as Fig. 5 from [1].

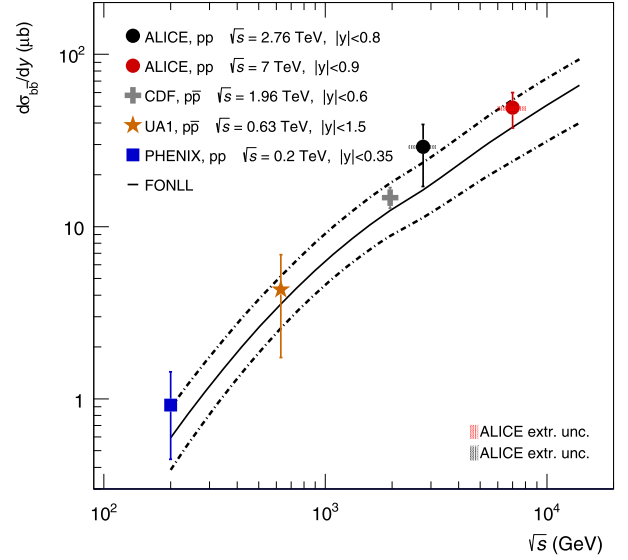


Fig. 7. This figure replaces Fig. 6 from [1]. Caption is the same as Fig. 6 from [1].

J/ψ mesons from beauty-hadron decays [5] is also updated. After subtracting the new cross section of the electrons from beauty-hadron decays from the measured cross section of the electrons from heavy-flavour hadron decays [6], the production cross section of electrons from charm-hadron decays was converted into a charm production cross section. The charm production cross section per unit rapidity at mid-rapidity ($d\sigma_{c\bar{c}}/dy$) and the total cross sections ($\sigma_{c\bar{c}}$) at $\sqrt{s} = 7$ TeV are also updated in Table 2. Since the corresponding quantity at $\sqrt{s} = 2.76$ TeV was not explicitly evaluated in [1], there is no corresponding entry in Table 2. All measured cross sections for 7 TeV (2.76 TeV) have an additional normalization uncertainty of 3.5% (1.9%) [7].

In Figs. 3, 4, 5, 6 and 7, we have updated accordingly the ALICE data points.

The main conclusion of the original papers remains valid: the data and predictions are consistent within the experimental and theoretical uncertainties.

References

- [1] B. Abelev, et al., ALICE Collaboration, Phys. Lett. B 738 (2014) 97.
- [2] B. Abelev, et al., ALICE Collaboration, Phys. Lett. B 721 (2013) 13.
- [3] K. Aamodt, et al., ALICE Collaboration, J. High Energy Phys. 01 (2012) 128.
- [4] B. Abelev, et al., ALICE Collaboration, J. High Energy Phys. 1207 (2012) 191, arXiv:1205.4007 [hep-ex].
- [5] B. Abelev, et al., ALICE Collaboration, J. High Energy Phys. 11 (2012) 1.
- [6] B. Abelev, et al., ALICE Collaboration, Phys. Rev. D 86 (2012) 112007, arXiv:1205.5423 [hep-ex].
- [7] B. Abelev, et al., ALICE Collaboration, Eur. Phys. J. C 73 (2013) 1.